

Correlation effects for semiconducting single wall carbon nanotube: a density matrix renormalization group study

Fei Ye,¹ Bing-Shen Wang,² Jizhong Lou,³ and Zhao-Bin Su³

¹Center for Advanced Study, Tsinghua University, Beijing 100084, China

²State Key Laboratory of Semiconductor Superlattice and Microstructure and Institute of Semiconductor, Academia Sinica, Beijing 100083, China

³Institute of Theoretical Physics, Academia Sinica, Beijing 100080, China

In this paper, we report the applicability of the density matrix renormalization group(DMRG) approach to the cylindrical single wall carbon nanotube (SWCN) for purpose of its correlation effect. By applying the DMRG approach to the $t+U+V$ model, with t and V being the hopping and Coulomb energies between the nearest neighboring sites, respectively, and U the onsite Coulomb energy, we calculate the phase diagram for the SWCN with chiral numbers ($n_1 = 3, n_2 = 2$), which reflects the competition between the correlation energy U and V . Within reasonable parameter ranges, we investigate possible correlated groundstates, the lowest excitations and the corresponding correlation functions in which the connection with the excitonic insulator is particularly addressed.

PACS numbers: 71.10.Fd, 71.10.Hf, 71.35.-y, 78.67.Ch

Since the discovery of carbon nanotube, many efforts, both experimental and theoretical, have been put into understanding the electron correlation effect, specially for thin single wall carbon nanotubes(SWCN). The transport as well as the angle-integrated photoemission^{1,2} studies on the bundles of SWCN show interesting evidence of the non-trivial correlation effects which are believed to be contributed by the metallic SWCNs and are consistent with the Tomonaga-Luttinger theory^{3,4,5}. For the semiconducting SWCNs, the discrepancy between the experimentally measured ratio of the absorption frequency to the emission frequency^{6,7} and that predicted by the tight binding approximation(TBA)⁸ is also attributed to the correlation effects in literatures^{9,10,11}. Theoretically, the correlation effect of SWCNs so far has been treated^{3,4,5,9,10,11,12,13,14} by *ab initio* numerical calculations, perturbative renormalization group(RG), and various improved or modified Hartree-Fock approximations(HFA). However in these approaches the strong correlation effects are not easy to be treated seriously.

It is known that the π -electron has its wave function extending perpendicular to the surface of SWCN⁸ with a weak overlap among themselves, so that its kinetic energy in a range of 2.4-3.2eV is much smaller than the onsite Coulomb energy about 11.76eV¹⁵ while the nearest neighboring(NN) Coulomb energy is also as big as an order of 5eV. Therefore the SWCN is a system which might exhibit strong correlation effect. We consider an extended Hubbard model to study the correlation physics of SWCNs

$$H = \sum_{\langle i,j \rangle} c_{i,\sigma}^\dagger c_{j,\sigma} + h.c. + U \sum_i n_{i,\uparrow} n_{i,\downarrow} + V \sum_{i,j} (n_i - 1)(n_j - 1), \quad (1)$$

where the hopping energy t is set to be unit, while U and V are onsite and NN Coulomb energies, respectively. c_i

and c_i^\dagger are the electron annihilation and creation operators with i the site index, respectively. The particle number operator for spin σ at site i is $n_{i,\sigma} = c_{i,\sigma}^\dagger c_{i,\sigma}$ and $n_i = n_{i,\uparrow} + n_{i,\downarrow}$. Here we neglect the curvature induced difference among the three hopping directions on each site. This minimal model has been studied in Refs.[4,14] for metallic tubes by perturbative RG and unrestricted HFA, respectively. It has also been applied to the graphite system¹⁶.

In this paper, we report the applicability of the DMRG approach to the cylindrical SWCN for purpose of studying its correlation effect. By applying this approach to the $t+U+V$ model Eq.(1), we compute the phase diagram for the SWCN with chiral numbers ($n_1 = 3, n_2 = 2$), which essentially reflects the competition between the correlation energies U and V . Within reasonable parameter ranges of U/t and V/t , we investigate possible correlated groundstates, the lowest excitations and the corresponding correlation functions.

As well accepted, the DMRG approach is an accurate and efficient treatment for the quasi-1D strongly correlated systems¹⁷. The main problem for the implementation of DMRG to the SWCN lies in how to construct an appropriate superblock configuration for such a cylindrically warped hexagonal lattice sheet. We notice that, following the literature[18], for a given pair of chiral numbers (n_1, n_2) with N the greatest common divisor, the corresponding SWCN can be constructed by successive piling of motifs along the tube axis conducted by a screw operation¹⁸, where each motif contains N unit cells in coincidence with the N -fold rotational symmetry of the tube. This implies an N -multiple helical structure hidden in the SWCN. The unit cells are labelled by two integers (m, l) with $l = 1, 2, \dots, N$ which corresponds the l -th cell in the m -th motif. The two carbon atoms in one unit cell are distinguished by an index $\nu = A, B$. Based upon the above observation, we map such N -multiple helical SWCN onto a $2N$ chain lattice

so as to make the DMRG procedure can be straightforwardly implemented. In this helical coordinate system, the site (m, l, A) has NNs labelled by (m, l, B) , $(m - \frac{n_1}{N}, l + p_1, B)$, $(m + \frac{n_2}{N}, l - p_2, B)$, where p_1, p_2 are integer solutions of equation $n_1 p_2 - n_2 p_1 = N^{18}$. In particular, for case of $N = 1$, which is the most advantaged, all the unit cells on the tube can be threaded by only one helical curve and l becomes a dummy index. Then the Hamiltonian in Eq.(1) can be rigorously mapped to a twisted two-chain model with finite long range hoppings as $H = H_t + H_U + H_V$ with

$$\begin{aligned} H_t &= \sum_{m, \mu \in \mathcal{S}} \sum_{\sigma} c_{m, \sigma}^{A\dagger} c_{m+\mu, \sigma}^B + h.c. \\ H_U &= U \sum_{m, \nu=A, B} n_{m, \uparrow}^{\nu} n_{m, \downarrow}^{\nu} \\ H_V &= V \sum_{m, \mu \in \mathcal{S}} (n_m^A - 1)(n_{m+\mu}^B - 1) \end{aligned} \quad (2)$$

where $\mathcal{S} = \{0, -n_1, n_2\}$, $n_{m, \sigma}^{\nu} = c_{m, \sigma}^{\nu\dagger} c_{m, \sigma}^{\nu}$, $n_m^{\nu} = n_{m, \uparrow}^{\nu} + n_{m, \downarrow}^{\nu}$ and $c_{m, \sigma}^{\nu}$ is exactly the same operator $c_{i, \sigma}$ but with its index relabelled in terms of motif-cell labels. Fig. 1a and 1b show such a mapping for the tube ($n_1 = 3, n_2 = 2$) with $N = 1$.

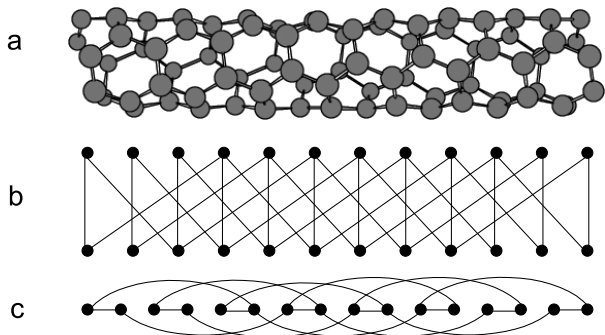


FIG. 1: Illustration for the mapping from a cylindrical SWCN(1a) with index (3,2) to a twisted two chain model with finite long range hopping (1b), where the solid lines connect the NN pairs. For purpose of DMRG calculation, we further squeeze the two chains in (1b) into a single chain (1c) with A atom and B atom arranged alternatively, where the lines are kept with the same meaning as in (1b).

To extract most physical implications with small enough computing effort, in this paper, we apply the standard DMRG approach to the intrinsic semiconducting SWCN (3, 2) with $N = 1$, in which the open boundary condition(OBC) is engaged. The computed groundstate phase diagram is plotted in Fig. 2. It can be divided into three phases as the *excitonic insulator*(E), *normal semiconductor*(N), and *Mott insulator*(M), as will be clear shortly.

For our minimal model as Eq.(2) when both U and V are small, the system is a semiconductor which can

be divided into two regions N_s and N_T according to the first excitations. The boundary between them is shown

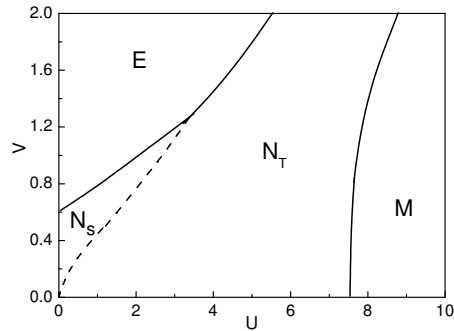


FIG. 2: The phase diagram of semiconducting SWCN(3,2). See the text for details.

as the dashed line in Fig. 2, across which a level crossing takes place for the gapped excited states with different spin symmetries, i.e., the singlet in the N_s region and the triplet in the N_T region, which are favored by V and U , respectively. We interpret these excitations in connection with the singlet and triplet excitons for the intrinsic semiconducting SWCN. The groundstate in these two regions is a non-degenerate singlet state, of which the equal time correlation function(ETCF) is exponentially decaying in both spin and charge sectors. The difference is that density-density correlation is much stronger than the spin-spin correlation in the N_s region and vice versa in the N_T region.

If we still keep U small but increase V , the first spin singlet excitation would get lowered. When it reaches the groundstate, the system then undergoes a transition into a new phase in association with the excitonic insulator¹⁹. As a consequence of the “fallen state”, there are two mutually orthogonal degenerate groundstates in the E phase as $|G_+^{(E)}\rangle$ and $|G_-^{(E)}\rangle$, in which the 2-fold degeneracy is understood in the thermodynamic limit. Both of them are spin singlet and eigenstates of the parity, belonging to eigenvalues ± 1 , respectively. Moreover, the amplitude of the density-density correlation increases with increasing V as shown in the upper panel of Fig. 3, until into the E phase it is identical for both the two degenerate groundstates and no longer decays. This non-decaying correlation could be interpreted as the existence of a charge density wave in the two groundstates. When computing the matrix element of the particle number operator n_m^{ν} between these two degenerate states, it is found that the diagonal term $\langle G_+^{(E)} | n_m^{\nu} | G_+^{(E)} \rangle$ (or $\langle G_-^{(E)} | n_m^{\nu} | G_-^{(E)} \rangle$) is trivially equal to 1, but the off-diagonal matrix element is

$$\langle G_+^{(E)} | n_m^{\nu} | G_-^{(E)} \rangle \sim (-1)^{\nu} \tilde{n} \quad (3)$$

with \tilde{n} being a site-independent constant and $(-1)^{\nu} = \pm 1$ for $\nu = A, B$, respectively. By mixing the two states

$|G_{\pm}^{(E)}\rangle$, one can construct the groundstate with alternative density distribution in the A and B sublattices. This can be viewed as the exciton (particle-hole pair) condensation in the groundstate of E phase with a spontaneous symmetry breaking between the sublattices.

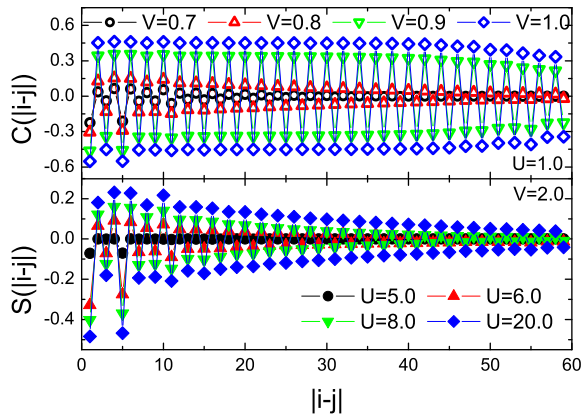


FIG. 3: The charge and spin correlation functions. The coordinate system for the horizontal axis is explained in Fig. 1c. The origin is set on the atom A in the middle cell of the tube. The data are obtained by keeping 2000 states and with 1-2 finite size sweep to get convergent results. The upper panel gives the change of charge correlation $C(|i-j|)$ with respect to V for fixed $U = 1.0$ and the lower panel is the antiferromagnetic spin correlation $S(|i-j|)$ for different U with fixed $V = 2.0$.

Starting from the region N_T , if we further increase U , the triplet first excitation would be lowered continuously with the groundstate spin-spin ETCF growing. In the lower panel of Fig. 3, we show the variation of spin correlation versus U for fixed value of V . Until some critical value of $U = U_c$, the triplet spin gap vanishes in the thermodynamic limit²¹, and a transition from phase N to the Mott phase M takes place. In the Mott phase, besides a finite charge gap the system develops gapless spin wave type excitations. The Mott phase is far from the possible realistic parameter region of U and V for the SWCN(3,2), however it may be realized in the small gap semiconductor or metallic tube.

The phase boundaries in Fig. 2 are scanned by computing the energy gap in the particle-hole channel for various U and V . In this procedure, we adopt the infinite algorithm with 1000 states being kept and then extrapolate the finite size data to the thermodynamic limit. The calculated phase boundaries will also be checked by other independent method below. In Fig. 4, we give the variation of the gap with respect to U for some fixed values of V as examples.

For $V = 2$ in Fig. 4a, the 2-fold degeneracy of the groundstates in E phase is lifted abruptly at the $E - N_T$ phase boundary $U_C = 5.6$ and a finite spin triplet

excitation gap is opened. It decreases with increasing U and vanishes at about $U = 8.8$. Fig. 4b with $V = 0.8$ shows a different picture. The singlet gap emerges gradually from zero at the $E - N_s$ phase boundary. When

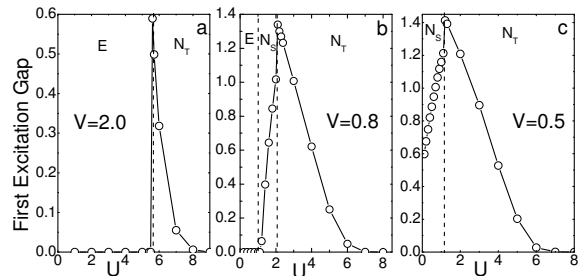


FIG. 4: The first excitation gap as a function of onsite Coulomb potential U , for $V = 2.0$ in (4a), $V = 0.8$ in (4b), and $V = 0.5$ in (4c). The vertical dashed lines indicate the transition points.

the increasing U reaches the $N_s - N_T$ boundary, a level crossing takes place from the singlet excitation to the triplet excitation. Fig. 4c with $V = 0.5$ only shows a $N_s - N_T$ transition qualitatively the same as that in Fig. 4b.

To further explore the nature of the above shown phase boundaries, and in particular, as an independent check, we compute the average of double occupancy and the NN density correlation over the groundstate, denoted by δ and ρ , respectively, as in Ref.[20]

$$\begin{aligned} \delta &\equiv \partial E_{GS} / \partial U = (H_U / UL) \\ \rho &\equiv \partial E_{GS} / \partial V = (H_V / VL) . \end{aligned} \quad (4)$$

Here E_{GS} is the groundstate energy per site and the Hellmann-Feynman theorem is applied. For fixed $V = 2.0$ or 0.8 , the δ and ρ as functions of U are plotted in Fig. 5. The calculations are performed on the tube with 120, 160 and 200 carbon atoms by keeping 2000 states and sweeping 1-2 times to get convergent results. The results calculated from different atom numbers coincide with one another nicely, which provides a strong evidence that the calculated main features of the transition will survive in the thermodynamic limit.

As shown in the right panel in Fig. 5, there is an abrupt jump for both δ and ρ at the critical point $V = 2.0$ and $U = 5.6$. It indicates the phase boundary between E and N_T belongs to the first order transition. Note that the phase boundaries (dashed lines) in Fig. 5 are extracted from the phase diagram Fig. 2, which agree with the data of δ and ρ very well. If we further increase U from region N_T to phase M , δ and ρ vary smoothly across the phase boundary (see also right panel of Fig. 5). It is understood that the $N_T - M$ phase transition is of the Kosterlitz-Thouless type without symmetry breaking, where the N_T region with a gapful (massive) triplet excitation spectrum transits into the M phase with gapless (massless) spin ex-

citations. In the left panel of Fig. 5, there is a discontinuity in the slope of both δ and ρ as functions of U on the $N_s - E$ phase boundary, which means this boundary belongs to a second order phase transition. Across the $N_s - N_T$ division line, a level crossing of the excited states, not a phase transition, takes place.

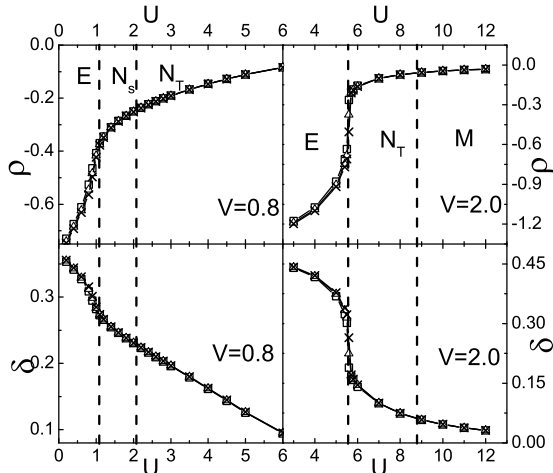


FIG. 5: The plot of δ and ρ as functions of U for fixed V . The vertical dashed lines indicate the transition points which are extracted from the phase diagram Fig. 2. The calculated data are for 120 atoms (open squares), 160 atoms (open triangles), and 200 atoms (cross symbol), respectively.

Briefly the transitions from the semiconductor into the excitonic insulator and Mott insulator take place whenever the band gap is overwhelmed completely by V and U , respectively. For other semiconducting SWCNs, the augment of the tube diameter will reduce the TBA band gap, which will consequently shift the phase boundaries $E - N_s$ and $N_T - M$. However the phase boundaries $E - N_T$ and $N_s - N_T$ should not change too much because they can be viewed as the balance position of the competition between U and V .

In our minimal model, the longer range (LR) part of Coulomb interaction is ignored, which is nonessential in describing the correlated groundstate of semiconducting SWCNs. Since we are dealing with the low energy excitations of the intrinsic semiconducting SWCN, the main effects of the LR Coulomb interaction are confined in the forming particle-hole excitations and its remnant effect leads to a renormalization of U and V . Based on the above argument, the groundstate of SWCN may be an excitonic insulator, normal semiconductor with different type of first excitations and Mott insulator, which is dependent on the chiral structure of SWCN and also the environment. In experiments, people can realize the transition of the correlated groundstate of SWCNs by applying a uniform pressure or by changing the band gap via the magnetic flux^{22,23,24}.

Acknowledgement: We thank sincerely to Profs. S.J.Qin, E.Tosatti, T.Xiang and L.Yu for beneficial discussions.

- ¹ M. Bockrath, *et al.*, Nature(London) **397**, 598(1999)
- ² H. Ishii, *et al.*, Nature(London) **426**, 540(2003).
- ³ L. Balents and M. P. A. Fisher, Phys. Rev. B **55**, R11973(1997)
- ⁴ Yu. A. Krotov, D. H. Lee, and S. G. Louie, Phys. Rev. Lett. **78**, 4245(1997)
- ⁵ C. Kane, L. Balents and M. P. A. Fisher, Phys. Rev. Lett. **79**, 5086(1997)
- ⁶ M. J. O'Connell, *et al.*, Science **297**, 593(2002).
- ⁷ S. M. Bachilo, *et al.*, Science **298**, 2361(2002).
- ⁸ S. Saito, G.Dresselhaus and M. S. Dresselhaus, *Physical Properties of Carbon Nanotube*(Imperial College Press, London, 1998)
- ⁹ C. L. Kane and E. J. Mele, Phys. Rev. Lett. **90**, 207401(2003)
- ¹⁰ C. D. Spataru, S. Ismail-Beigi, L. X. Benedict, and S. G. Louie, Phys. Rev. Lett. **92**, 077402(2004).
- ¹¹ H. Zhao and S. Mazumdar, Phys. Rev. Lett. **93**, 157402(2004)
- ¹² T. Ando, J. Phys. Soc. Jpn. **66**, 1066(1997).
- ¹³ E. Chang, G. Bussi, A. Ruini, and E. Molinari, Phys. Rev. Lett. **92**, 196401(2004).
- ¹⁴ M. P. Lopez Sancho, M. C. Munoz, and L. Chico, Phys. Rev. B **63**, 165419(2001)
- ¹⁵ W. A. Harrison, Phys. Rev. B **31**, 2121(1985).
- ¹⁶ Andrei L. Tchougreeff and R. Hoffmann, *et al.*, J. Phys. Chem. **96**, 8993(1992).
- ¹⁷ S. R. White, Phys. Rev. Lett. **69**, 2863(1992); Phys. Rev. B **48**, 10345(1993); U. Schollwöck, cond-mat/0409292
- ¹⁸ C. T. White, D. H. Robertson, and J. W. Mintmire, Phys. Rev. B **47**, R5485(1993); M. Damnjanović, *et al.*, Phys. Rev. B, **60**, 2728(1999)
- ¹⁹ D. Jerome, T. M. Rice, and W. Kohn, Phys. Rev. **158**, 462(1967)
- ²⁰ E. Jeckelmann, Phys. Rev. Lett. **89**, 236401(2002)
- ²¹ The finite size algorithm with 2000 states kept is used to calculate the spin gap in the particle-hole channel up to 200 carbon atoms in the *Mott* phase. The gap value extrapolated to the thermodynamic limit is around $\sim 10^{-4}$, which can be viewed as zero.
- ²² H. Ajiki and T. Ando, J. Phys. Soc. Jpn. **65**, 505(1996).
- ²³ J. P. Lu, Phys. Rev. Lett. **74**, 1123(1995).
- ²⁴ S. Zaric, *et al.*, Science **304**, 1129 (2004); U.C. Coskun, *et al.*, Science **304**, 1132 (2004)